Submitted to the
22nd International Symposium on Lepton-Photon Interactions at High Energy
June 30 – July 5, 2005; Uppsala, Sweden

Abstract: 286 **Session: QCD/HS**

Event shapes in deep inelastic $ep \to eX$ scattering at HERA

ZEUS Collaboration

Abstract

Means and differential distributions of event-shape variables have been studied in neutral current deep inelastic scattering using an integrated luminosity of 82.2 pb^{-1} collected with the ZEUS detector at HERA. The kinematic range used was $80 < Q^2 < 2 \cdot 10^4\,\mathrm{GeV}^2$ and $0.0024 < x < 0.6$, where Q^2 is the virtuality of the exchanged boson and x is the Bjorken variable. The Q-dependence of the means and distributions of the shape variables are compared with a model based on fixed-order plus next-to-leading-logarithm perturbative calculations and the Dokshitzer-Webber non-perturbative corrections ('power corrections').

1 Introduction

Event-shape variables, which give information about the topology of the hadronic final state, are sensitive to the strong coupling constant, α_s. Event-shape studies have been made by e^+e^- [1–3] and ep [4,5] experiments. However, there are two significant difficulties when testing QCD using these variables. Firstly, they are subject to large hadronization corrections. Secondly, the perturbative series do not strongly converge at low values of the shape variables [6]. Hadronisation can be described by a power correction (PC) of the type proposed by Y. Dokshitzer and B. Webber [7] where hadronization is described by two parameters: the perturbative parameter α_s and the non-perturbative parameter $\overline{\alpha_0}$. To deal with the lack of convergence at low values of the shape variables, it is necessary either to consider an observable which is not strongly affected, such as the mean of an event-shape variable, or to include higher-order terms in the calculations.

The ZEUS Collaboration has previously published results on mean event shapes, which suggested that higher-order corrections were necessary [5]. The H1 Collaboration has also previously published results on mean event shapes [4]. In this paper, the mean event-shape variables are revisited with a larger data sample. In addition, fits to differential event-shape data are presented and compared to next-to-leading-logarithm (NLL) resummed calculations matched to next-to-leading-order (NLO) QCD. A new event shape variable, K_{OUT}, is examined.

2 Detector description

The analysis is based on an inclusive sample of neutral current deep inelastic scattering (DIS) events collected with the ZEUS detector during the 1998-2000 running period at HERA, corresponding to an integrated luminosity of 82.2 pb^{-1}.

A detailed description of the ZEUS detector can be found elsewhere [8]. A brief outline of the components that are most relevant for this analysis is given below. The high-resolution uranium–scintillator calorimeter (CAL) [9] consists of three parts: the forward (FCAL), the barrel (BCAL) and the rear (RCAL) calorimeters. Each part is subdivided transversely into towers and longitudinally into one electromagnetic section (EMC) and either one (in RCAL) or two (in BCAL and FCAL) hadronic sections (HAC). The smallest subdivision of the calorimeter is called a cell. The CAL energy resolutions, as measured under test-beam conditions, are $\sigma(E)/E = 0.18/\sqrt{E}$ for electrons and

$\sigma(E)/E = 0.35/\sqrt{E}$ for hadrons (E in GeV). Charged particles are tracked in the central tracking detector (CTD) [10], which operates in a magnetic field of 1.43 T provided by a thin superconducting coil. The CTD consists of 72 cylindrical drift chamber layers, organized in 9 superlayers covering the polar-angle region $15^\circ < \theta < 164^\circ$. The transverse-momentum resolution for full-length tracks is $\sigma(p_T)/p_T = 0.0058 p_T \oplus 0.0065 \oplus 0.0014/p_T$, with p_T in GeV.

The scattered positron identification algorithm was based on a neural network [11] which uses information from the CAL. The final state particles in the reaction $ep \to eX$ were reconstructed from the tracks and calorimeter energy deposits. The DIS kinematic variables and the four-vector of the virtual photon were reconstructed using the double-angle (DA) method [12]. The momenta, $\left(\overrightarrow{p},\ \ E\right)$, of the particles of the system X were reconstructed from calorimeter clusters and from tracks in the CTD [5, 13].

3 Event-shape variables

The event-shape variables studied here are thrust, jet broadening, the invariant jet mass, the C-parameter and the momentum out of the event plane.

Thrust measures the longitudinal collimation of a given hadronic system, while broadening measures the complementary aspect. These two parameters are specified relative to a chosen axis, denoted by a unit vector $\boldsymbol{n}$. Thus:

$$T = \frac{\sum_i |\overrightarrow{p_i} \cdot \overrightarrow{n}|}{\sum_i |\overrightarrow{p_i}|}; \tag{1}$$

$$B = \frac{\sum_i |\overrightarrow{p_i} \times \overrightarrow{n}|}{\sum_i |\overrightarrow{p_i}|}. \tag{2}$$

The shape parameters in Equations (1)–(4) are summed over the particles in the current hemisphere of the Breit frame. With $\boldsymbol{n}$ taken to be the virtual-photon direction, thrust and broadening are denoted by T_γ and B_γ, respectively. Alternatively, both quantities may be measured with respect to the thrust axis, defined as that direction along which the thrust is maximised by a suitable choice of $\boldsymbol{n}$. In this case, the thrust and broadening are denoted by T_T and B_T.

The normalised jet invariant mass, M, is defined by

$$M^2 = \frac{\left(\sum_i E_i\right)^2 - \left|\sum_i \overrightarrow{p_i}\right|^2}{\left(2\sum_i E_i\right)^2}. \tag{3}$$

The C-parameter is given by

$$C = \frac{3\sum_{ij} |\overrightarrow{p_i}||\overrightarrow{p_j}| \sin^2(\theta_{ij})}{2(\sum_i |\overrightarrow{p_i}|)^2}, \tag{4}$$

where θ_{ij} is the angle between two final state particles, i and j.

The momentum out of the event plane is given by [14]:

$$K_{OUT} = \sum_i \left|\overrightarrow{p_i^{out}}\right|. \tag{5}$$

The $\overrightarrow{p_i^{out}}$ is the component of momentum of the hadron i perpendicular to the *event plane* defined by the proton momentum $\overrightarrow{P}$ in the Breit frame and the unit vector $\overrightarrow{n}$ which enters the definition of thrust major:

$$T_M = \max \frac{\sum_i |\overrightarrow{p_i} \cdot \overrightarrow{n}|}{\sum_i |\overrightarrow{p_i}|}, \ \overrightarrow{P} \cdot \overrightarrow{n} = 0. \tag{6}$$

The sum in Equations (5) and (6) runs over all particles in the Breit frame.

As seen from the above equations, the shape parameters in Equations (1)–(4) are normalised to the energy in the current hemisphere of the Breit frame. With this normalisation, to ensure infra-red safety, it is necessary to exclude events in which the energy in the current hemisphere is less than a certain limit, $\mathcal{E}_{lim}$. A value of $\mathcal{E}_{lim} = 0.25Q$ has been used. The analysis is based on event shapes calculated in the P-scheme, i.e. with particles taken to have zero mass after boosting to the Breit frame.

In the Born approximation, T_γ and T_T are unity. Consequently, the shape variables $(1-T_\gamma)$ and $(1-T_T)$ are employed so that non-zero values at the parton level are a direct indicator of higher-order QCD effects.

4 Event selection and analysis

The selection and kinematic variable reconstruction follow those of a previous analysis [5]. The kinematic region used was $80 < Q^2 < 2 \cdot 10^4\,\mathrm{GeV}^2$ and $0.0024 < x < 0.6$ [5] for all

the variables except K_{OUT}, where $Q^2 > 100\,\mathrm{GeV}^2$.

Hadronic energy-flow objects, combining tracking information with calorimetry, were used to determine the event shapes [5, 13]. Bin-by-bin correction factors were calculated using a Monte Carlo sample of neutral current DIS events, generated using DJANGOH [15] with the Colour Dipole Model, as implemented in ARIADNE [16]. Systematic errors were estimated by changing the event selections and replacing ARIADNE by HERWIG [17] or LEPTO [18].

The mean event shapes have been fitted to NLO fixed-order QCD predictions and power corrections (see below). In addition, the distributions have also been fitted to NLO + NLL plus power corrections. The fitted parameters were $\alpha_s(M_Z)$, the strong coupling constant, and $\overline{\alpha_0}(\mu_I = 2\,\mathrm{GeV})$, the non-perturbative parameter introduced by the power correction. Statistical and experimental systematic errors were included in the fits using the Hessian method [19].

The means were fitted using a sample of 10^8 events generated with DISASTER++ [20] using the CTEQ4M [21] sets for the parameterizations of the proton parton densities (PDFs). To fit the differential distributions, 2×10^9 DISASTER++ events were generated using the DISPATCH [22] program with the MRST99 [23] PDFs. The power correction and matched NLL resummation were calculated using the DISRESUM [22] package. In DISRESUM, the power correction is applied as a shift of the distribution. The shift has the same functional form as the power correction for the mean. In the case of B_γ there is, in addition, a change in shape of the distribution. The modified M_2 matching scheme [24] was used as it minimised the dispersion in the fitted α_s and $\overline{\alpha_0}$ values between the variables. These calculations have not yet been done for K_{OUT}.

5 Results

5.1 Mean values

The NLO + PC calculation has been fitted to the mean values of the shape variables. The fitted and extracted parameters are shown in Fig. 1. For all variables, except $1 - T_\gamma$, the $\overline{\alpha_0}$ value obtained from the fit is consistently 0.45 ± 0.045. The value determined from $1 - T_\gamma$ is 35% lower. The value of α_s obtained from the fit is consistent for all variables except for B_T, which is 5% lower. This discrepancy cannot be explained by experimental uncertainties. The dispersion of the fitted α_s and $\overline{\alpha_0}$ values could be due to higher-order

terms that are not present in the NLO +PC calulations.

5.2 Differential distributions

Due to the lack of convergence of the perturbative series for the differential distributions, the NLO + PC model used for the mean is not expected to describe the distributions. For the distributions a resummation and matching is required. This is incorporated in the NLL + NLO + PC model used here. The results of the NLO + NLL + PC calculations fitted to the differential distributions are shown in Fig. 2.

The range over which the fit was performed is defined by the region where the power corrections are valid and where the shape variable is below the leading order upper limit. The model gives a good description of the differential distribution for T_γ and B_γ over the full range of Q and over a substantial range of the shape variable; the χ^2/dof of the fit is close to unity. For the remaining variables the χ^2/dof is about 5. The fitted α_s values are consistent with the world average. With the exception of C, the $\overline{\alpha_0}$ values are consistent with those found for the means.

5.3 Two jet variables

The differential distributions of K_{OUT}/Q for two Q^2 ranges: $100 < Q^2 < 500\,\mathrm{GeV}^2$ and $500 < Q^2 < 800\,\mathrm{GeV}^2$ are presented in Fig. 3. The data are described well by both LEPTO and ARIADNE. The first comparison with the LO + NLL + PC [25] is also shown. For the comparison, $\alpha_s = 0.118$, $\overline{\alpha_0} = 0.52$, and only the high Q^2 range is used. Since K_{OUT} is a two jet event-shape variable, the DISENT or DISASTER++ calculations can only give the first order prediction for this variable. A more precise comparison with the data would require a NLO calculation of order $\mathrm{O}(\alpha_s^3)$, e.g. NLOJET, and the corresponding next-to-leading-logarithm (NLL) calculations.

6 Conclusions

Existing ZEUS event-shape measurements are complemented by a new measurement of the means, using a larger data sample, and by measurements of differential distributions. For the kinematic ranges and cuts employed by this analysis, the NLO + PC calculation is unable to extract consistent results for all of the mean values and differential distributions

of the event-shape variables. When matched NLL resummations are added to the model, good fits to the differential distributions are obtained that yield $\alpha_s(M_Z)$ values that are consistent with the world average. For the first time, ZEUS has measured a two jet event-shape variable, K_{OUT}.

References

[1] DELPHI Coll., P. Abreu et al., Z. Phys. **C 73**, 229 (1997);
DELPHI Coll., P. Abreu et al., Phys. Lett. **B 456** (1999).

[2] P.A. Movilla Fernández et al. and the JADE Coll., Eur. Phys. J. **C 1**, 461 (1998);
JADE Coll.. O. Biebel et al., Phys. Lett. **B 459**, 326 (1999).

[3] P.A. Movilla Fernández et al., Comp. Phys. Comm. **C 22**, 1 (2001).

[4] H1 Coll., C. Adloff et al., Eur. Phys. J. **C 14**, 255 (2000);
H1 Coll., C. Adloff et al., Eur. Phys. J. **C 18**, 417 (2000).

[5] ZEUS Coll., S. Chekanov et al., Eur. Phys. J. **C 27**, 531 (2003).

[6] V. Antonelli,M. Dasgupta and G.P. Salam, JHEP **02**, 01 (2000).

[7] Yu.L. Dokshitzer and B.R. Webber, Phys. Lett. **B 352**, 451 (1997).

[8] ZEUS Coll., U. Holm (ed.), *The ZEUS Detector*. Status Report (unpublished), DESY (1993), available on `http://www-zeus.desy.de/bluebook/bluebook.html`.

[9] M. Derrick et al., Nucl. Inst. Meth. **A 309**, 77 (1991);
A. Andresen et al., Nucl. Inst. Meth. **A 309**, 101 (1991);
A. Caldwell et al., Nucl. Inst. Meth. **A 321**, 356 (1992);
A. Bernstein et al., Nucl. Inst. Meth. **A 336**, 23 (1993).

[10] N. Harnew et al., Nucl. Inst. Meth. **A 279**, 290 (1989);
B. Foster et al., Nucl. Phys. Proc. Suppl. **B 32**, 181 (1993);
B. Foster et al., Nucl. Inst. Meth. **A 338**, 254 (1994).

[11] H. Abramowicz, A. Caldwell and R. Sinkus, Nucl. Inst. Meth. **A 365**, 508 (1995).

[12] S. Bentvelsen, J. Engelen and P. Kooijman, *Proc. Workshop on Physics at HERA*, W. Buchmüller and G. Ingelman (eds.), Vol. 1, p. 23. Hamburg, Germany, DESY (1992).

[13] ZEUS Coll., J. Breitweg et al., Eur. Phys. J. **C 6**, 43 (1999).

[14] A. Banfi et al., Journal of High Energy Phys. **11**, 66 (2001).

[15] H. Spiesberger, HERACLES *and* DJANGOH*: Event Generation for ep Interactions at HERA Including Radiative Processes*, 1998, available on `http://www.desy.de/~hspiesb/djangoh.html`.

[16] L. Lönnblad, Comp. Phys. Comm. **71**, 15 (1992).

[17] G. Marchesini et al., Comp. Phys. Comm. **67**, 465 (1992).

[18] G. Ingelman, A. Edin and J. Rathsman, Comp. Phys. Comm. **101**, 108 (1997).

[19] D. Stump et al., Phys. Rev. **D 65**, 014012 (2002);
M. Botje, J. Phys. **G 28**, 779 (2002).

[20] D. Graudenz, Preprint hep-ph/9710244, 1997.

[21] H.L. Lai et al., Phys. Rev. **D 55**, 1280 (1997).

[22] M. Dasgupta and G.P. Salam, JHEP **0208**, 032 (2002).

[23] A.D. Martin et al., Eur. Phys. J. **C 14**, 133 (2000).

[24] M. Dasgupta and G.P. Salam, Eur. Phys. J. **C 24**, 213 (2002).

[25] G. Zanderighi, private communication, July 2004.

[26] S. Bethke, J. Phys. **G 26**, R27 (2000).

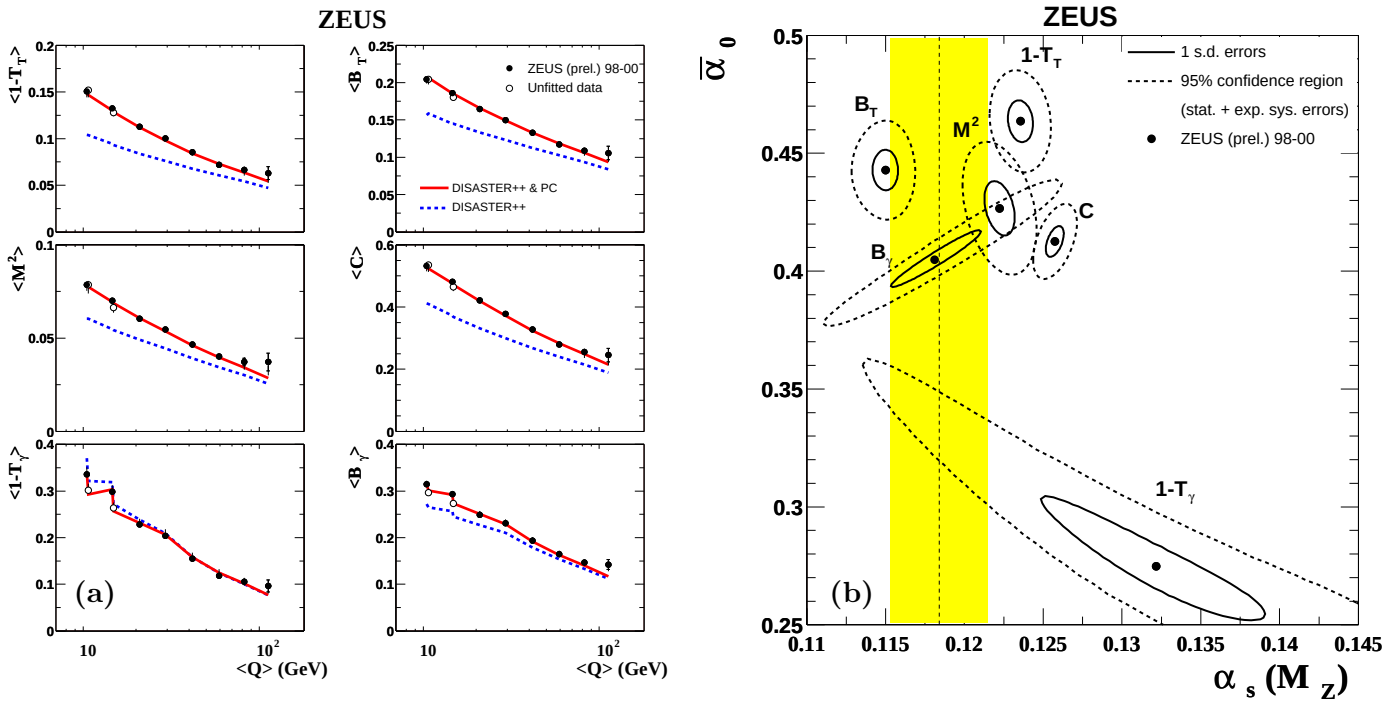

Figure 1: *The left plot shows the means of event shape variables matched to NLO + Power Correction. At low Q, there are two sets of points corresponding to different x-ranges. The lower points (open circles) were not used in the fit, although the final theoretical curves included these points producing a step shape in the low-Q region. The right plot shows the extracted parameter values. The vertical line and shaded area on the* $(\alpha_s, \overline{\alpha_0})$ *plot indicates the world average value of* $\alpha_s(M_Z)$ *[26].*

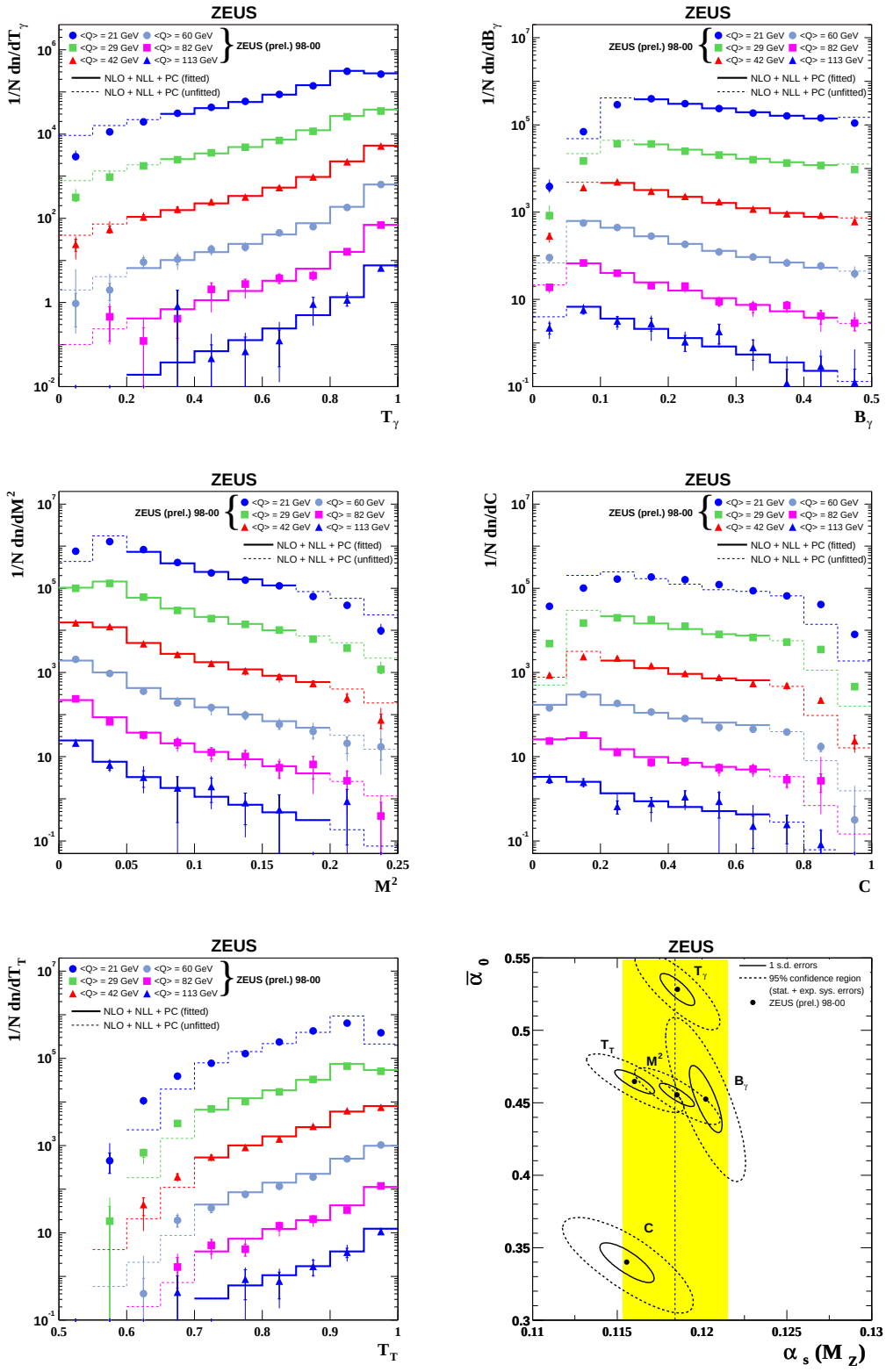

Figure 2: *Event shape distributions, fitted with NLL resummed calculations, matched to NLO + Power Corrections, and the extracted parameter values. The vertical line and shaded area on the* $(\alpha_s, \overline{\alpha_0})$ *plot indicates the world average value of* $\alpha_s(M_Z)$ *[26].*

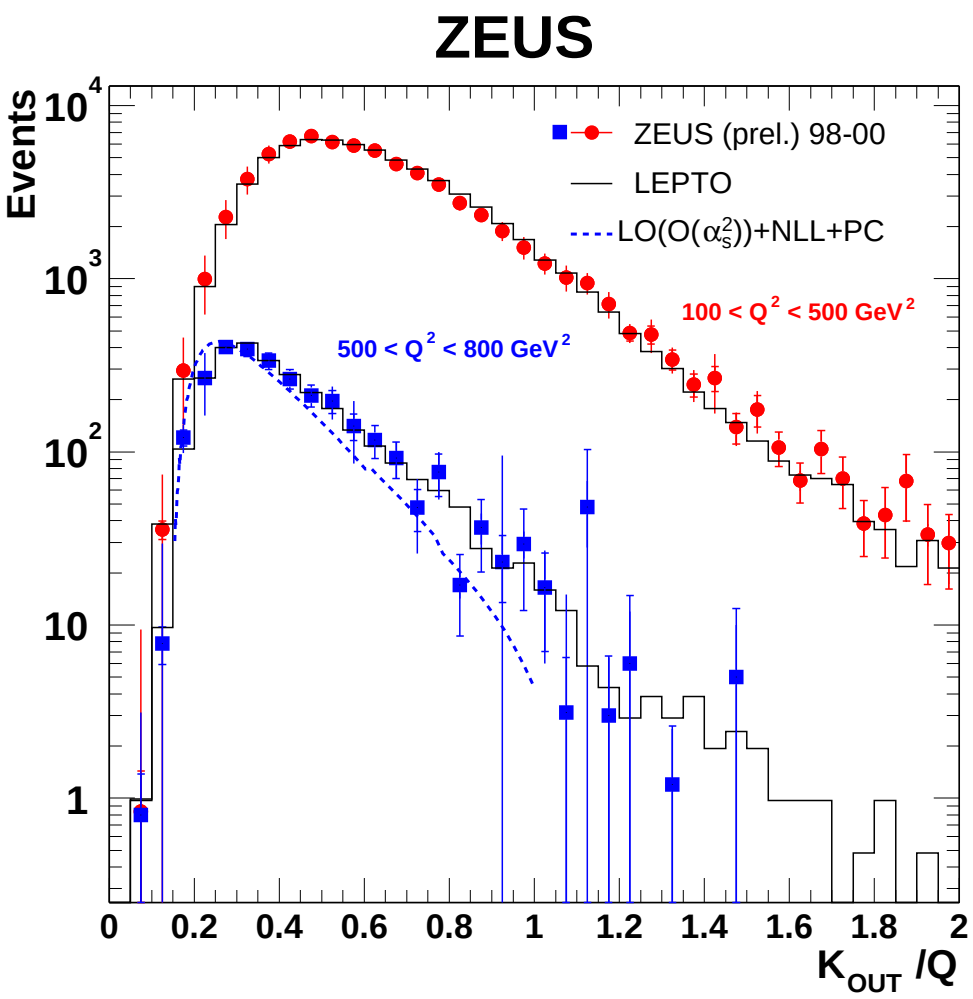

Figure 3: *Distribution of K_{OUT}/Q, corrected to the hadron level, compared to LEPTO and the LO + NLL + PC calculation shown for the Q^2 ranges $100\ GeV^2 < Q^2 < 500\ GeV^2$ and $500\ GeV^2 < Q^2 < 800\ GeV^2$. The inner error bars are statistical only; the outer error bars are statistical and systematic errors added in quadrature.*